

Supplementary information

Targeting the UFL1-AKT Cascade Suppresses Triple-Negative Breast Cancer Progression

Xiao Yang^{1,2*}, Yalei Wen^{2*}, Xiuqing Ma^{2*}, Shengying Qin^{3,4*}, Yixia Liu², Jiaqi Chen², Haoxing Zhang⁵, Colin R. Goding⁶, Rutao Cui^{7,8}, Tongzheng Liu^{1,2}

1. Department of General Surgery, Guangzhou Red Cross Hospital of Jinan University, Guangzhou, 510220, China

2. College of Pharmacy, Jinan University, Guangzhou, 510632, China

3. Department of Oncology, The First Affiliated Hospital of Jinan University, Guangzhou, 510630, China

4. Clinical Medical Research Institute, Jinan University, Guangzhou 510630, China

5. Guangdong Provincial Key Laboratory of Genome Stability and Disease Prevention, College of Life Sciences and Oceanography, Shenzhen University, Shenzhen, 518055, China

6. Ludwig Institute for Cancer Research, University of Oxford, Headington, Oxford OX3 7DQ, UK

7. Zhejiang University School of Medicine, Hangzhou, 310058, China

8. FuRong Laboratory, Changsha 410078, Hunan, China

*These authors contributed equally

Email: liutongzheng@jnu.edu.cn

| | |
|---|------|
| Supplementary Methods----- | 1-2 |
| Supplementary Fig 1-8 and figure legend----- | 3-15 |
| Supplementary Table 1. Pharmacokinetic Parameters after Intravenous Administration----- | 16 |
| Supplementary Table 2. Pharmacokinetic Parameters after Intraperitoneal Administration----- | 16 |

Supplementary Methods

Tandem affinity purification and mass spectrometry analyses

In brief, MDA-MB-231 cells were transfected with either a Flag-S-tagged empty vector or Flag-S-UFL1 construct. Cell pellets were lysed in NETN buffer (20 mM Tris-HCl pH 8.0, 300 mM NaCl, 0.5% NP-40, 1 mM EDTA) supplemented with protease and phosphatase inhibitors (Roche cocktail, 1 mM Na₃VO₄, 10 mM β-glycerophosphate, 1 mM PMSF, 10 mM NaF). For the first purification, cleared lysates were incubated with 20 μL Anti-Flag Affinity Gel (Sigma-Aldrich) for 2 h at 4°C. After three washes with NETN buffer, bound proteins were competitively eluted four times using 100 μg/mL 3×Flag peptide. The pooled eluates were diluted and subjected to a second purification with 50 μL S-protein agarose (Merck Millipore) for 4 h at 4°C, followed by three additional washes. The final immunoprecipitates were processed on-bead for MS analysis. Beads were resuspended in 6 M urea/PBS, reduced with 200 mM DTT (37°C, 30 min), and alkylated with 400 mM iodoacetamide (room temperature, 30 min in dark). After a PBS wash, proteins were digested overnight at 37°C with trypsin (1 μg) in 2 M urea/PBS containing 1 mM CaCl₂ and 50 mM NH₄HCO₃. Resulting peptides were collected, desalted using C18 columns, and dried. Samples were analyzed on an EASY-nLC 1200 HPLC system coupled to an Orbitrap Fusion Lumos mass spectrometer (Thermo Fisher Scientific). Raw data were processed with Proteome Discoverer 2.5 using a standard workflow. Searches were conducted against the *Homo sapiens* UniProt database (20,395 entries) with a mass tolerance of 4.5 ppm (MS) and 20 ppm (MS/MS). Two missed tryptic cleavages were permitted, and a reversed database was used to control the false discovery rate (FDR) at the site, peptide, and protein levels.

Far western blot

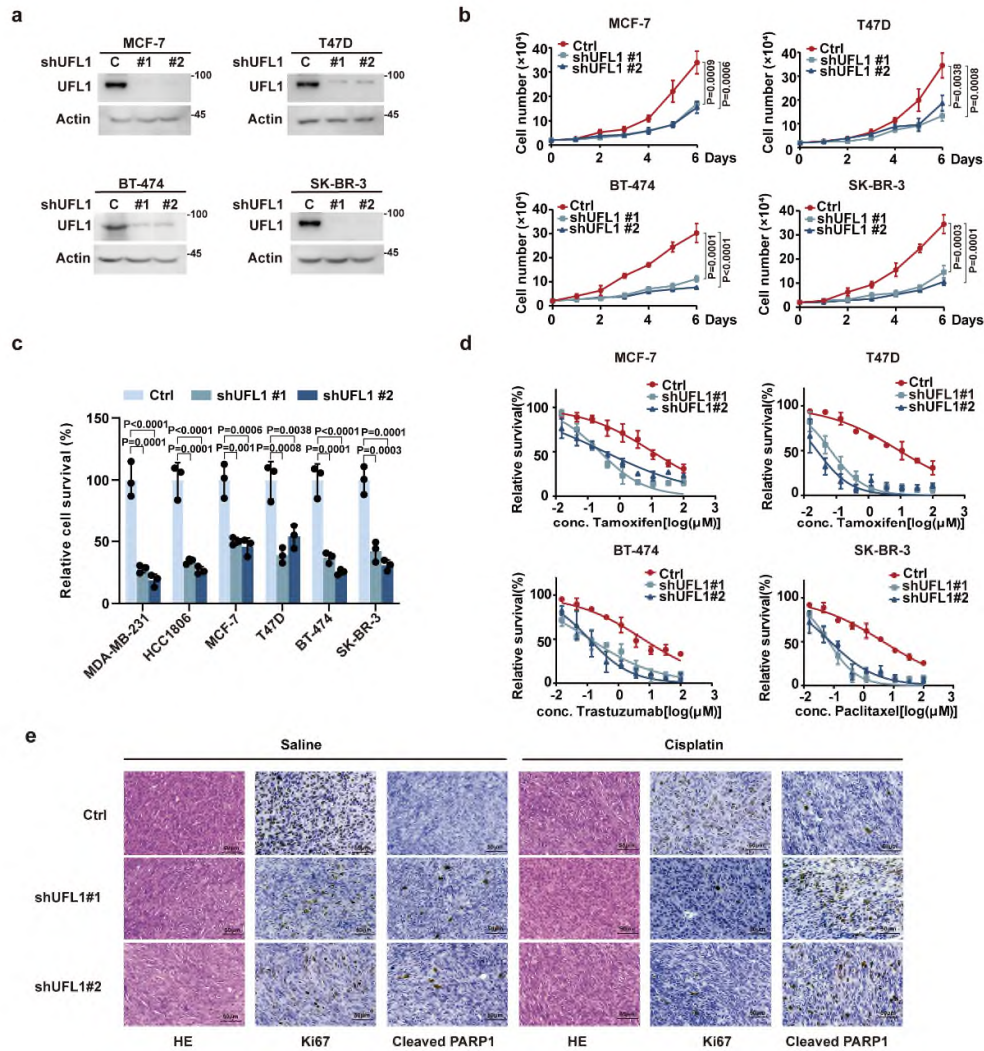
Far Western Blot was performed as described previously¹. Recombinant GST-AKT1 and His-tagged proteins (UBA5, UFC1, UFL1, UFBP1, UFM1 ΔC2) were expressed in *Escherichia coli* strain BL21 upon IPTG induction and purified using Glutathione Sepharose or Ni-NTA agarose, respectively. The purified proteins were mixed in a reaction buffer mentioned in the in vitro UFMylation assay and then separated by SDS-

PAGE.

Proteins were transferred onto polyvinylidene fluoride (PVDF) membranes (PVDF presoaked in methanol for 1 min). Membrane-bound proteins were renatured via sequential incubation in the denaturing and renaturing buffers (100 mM NaCl, 20 mM Tris pH 7.6, 0.5 mM EDTA, 10% glycerol, 0.1% Tween-20, 2% skim milk, 1 mM DTT) containing 6 M (30 min, RT), 3 M (30 min, RT), 0.1 M (30 min, 4°C), and 0 M (overnight, 4°C) guanidine-HCl. After blocking with 5% skim milk in PBST (4 mM KH₂PO₄, 16 mM Na₂HPO₄, 115 mM NaCl pH 7.4, 0.05% Tween-20) for 1 h at RT, membranes were incubated overnight at 4°C with purified Flag-mTOR proteins from cells (3 µg) in PBST buffer containing 3% milk at 4 °C overnight. Wash off un-bound mTOR with PBST buffer three times for 10 min and then incubated with the primary and secondary antibodies.

References

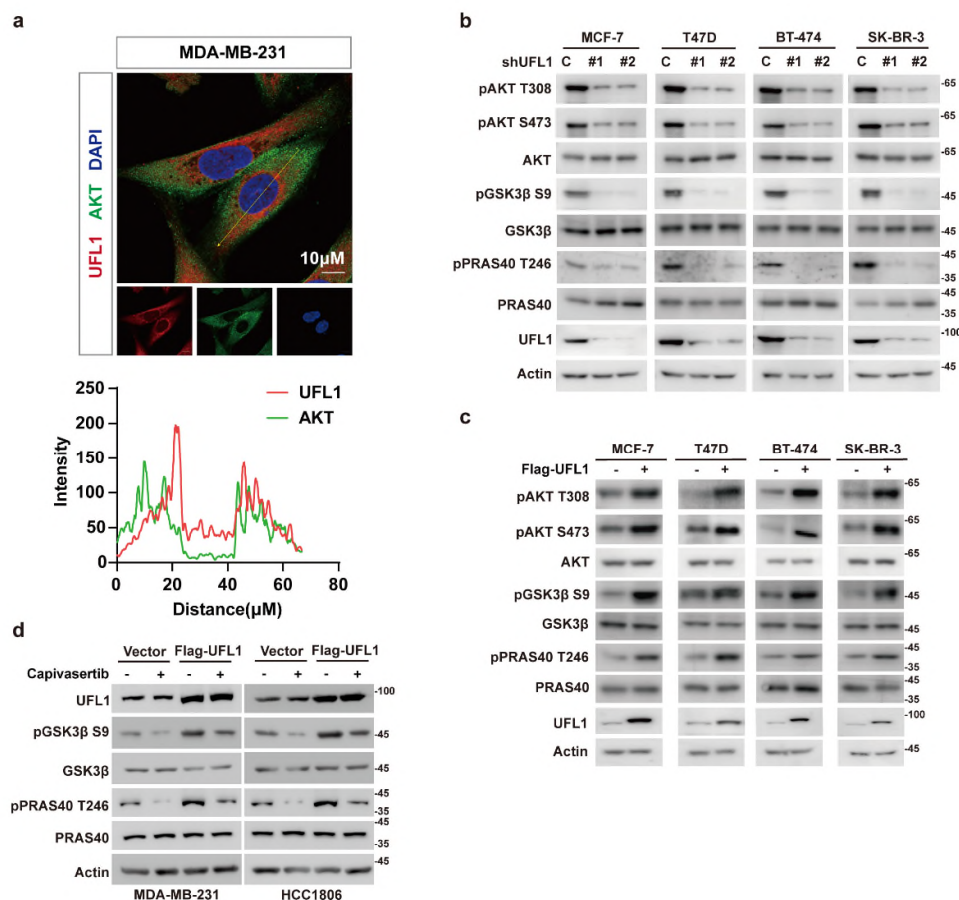
1. Wu, Y., Li, Q. & Chen, X.Z. Detecting protein-protein interactions by Far western blotting. *Nature protocols* **2**, 3278-3284 (2007).



Supplementary Fig. 1 UFL1 exerts an oncogenic role in breast cancer.

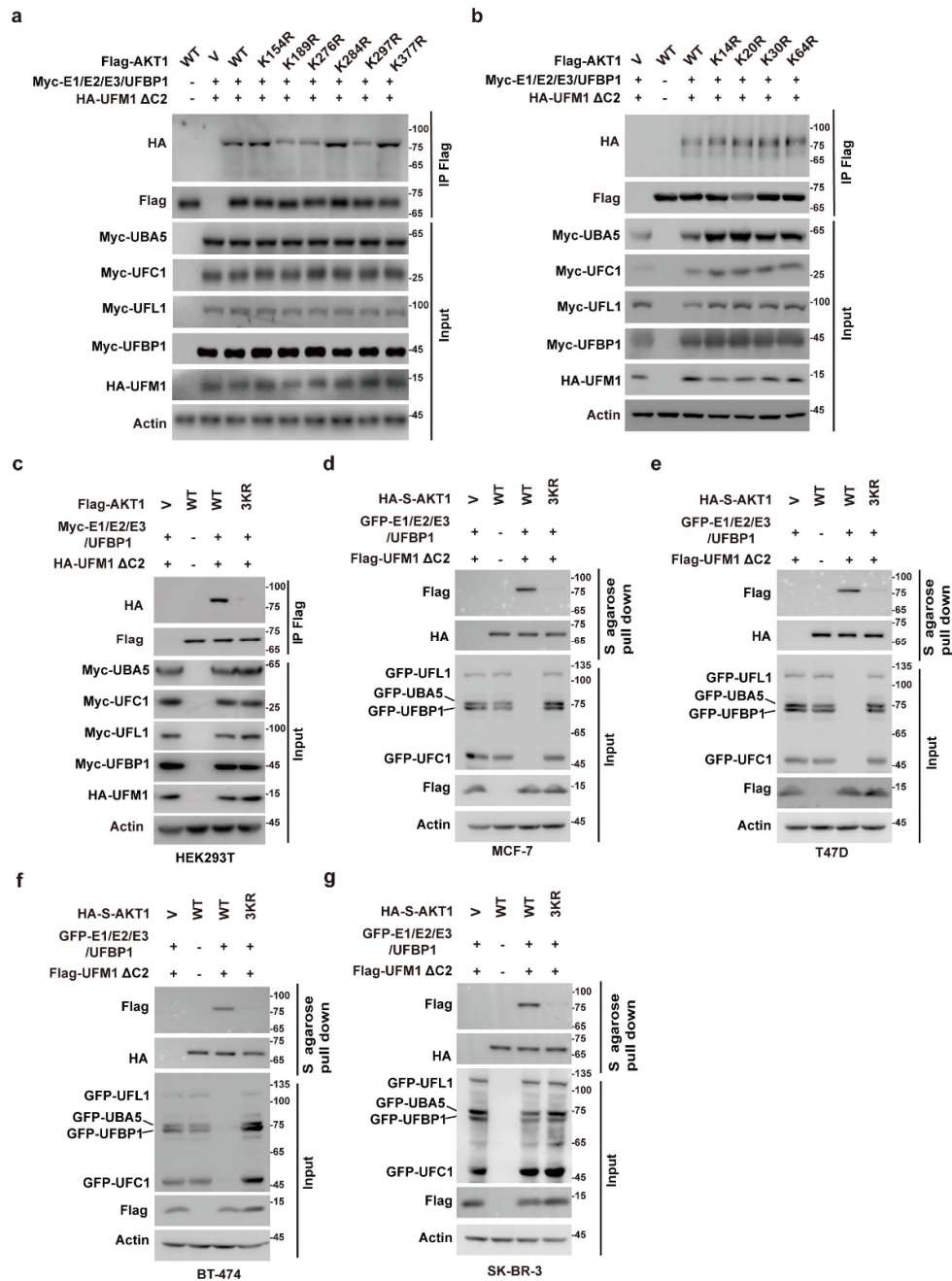
a, MCF-7, T47D, BT-474 and SK-BR-3 cells stably expressing control or UFL1 shRNAs were generated, and western blotting was performed using the indicated antibodies. **b**, Cell proliferation as in (a) was measured. **c**, Relative cell survival in various breast cancer cell lines (MDA-MB-231, HCC1806, MCF-7, T47D, BT-474, SK-BR-3) upon depletion of UFL1. **d**, MCF-7, T47D, BT-474 and SK-BR-3 cells stably expressing control or UFL1 shRNAs were treated with the indicated concentrations of tamoxifen, trastuzumab or paclitaxel and cell survival was determined. **e**, Representative images of H&E, Ki67 and cleaved PARP1 staining in xenograft models from (Fig. 1f). Data were presented as mean \pm SD of three independent experiments

(b-d). Data were analyzed by two-sided one-way ANOVA in **(b, c)**. Source data are provided as a Source Data file.



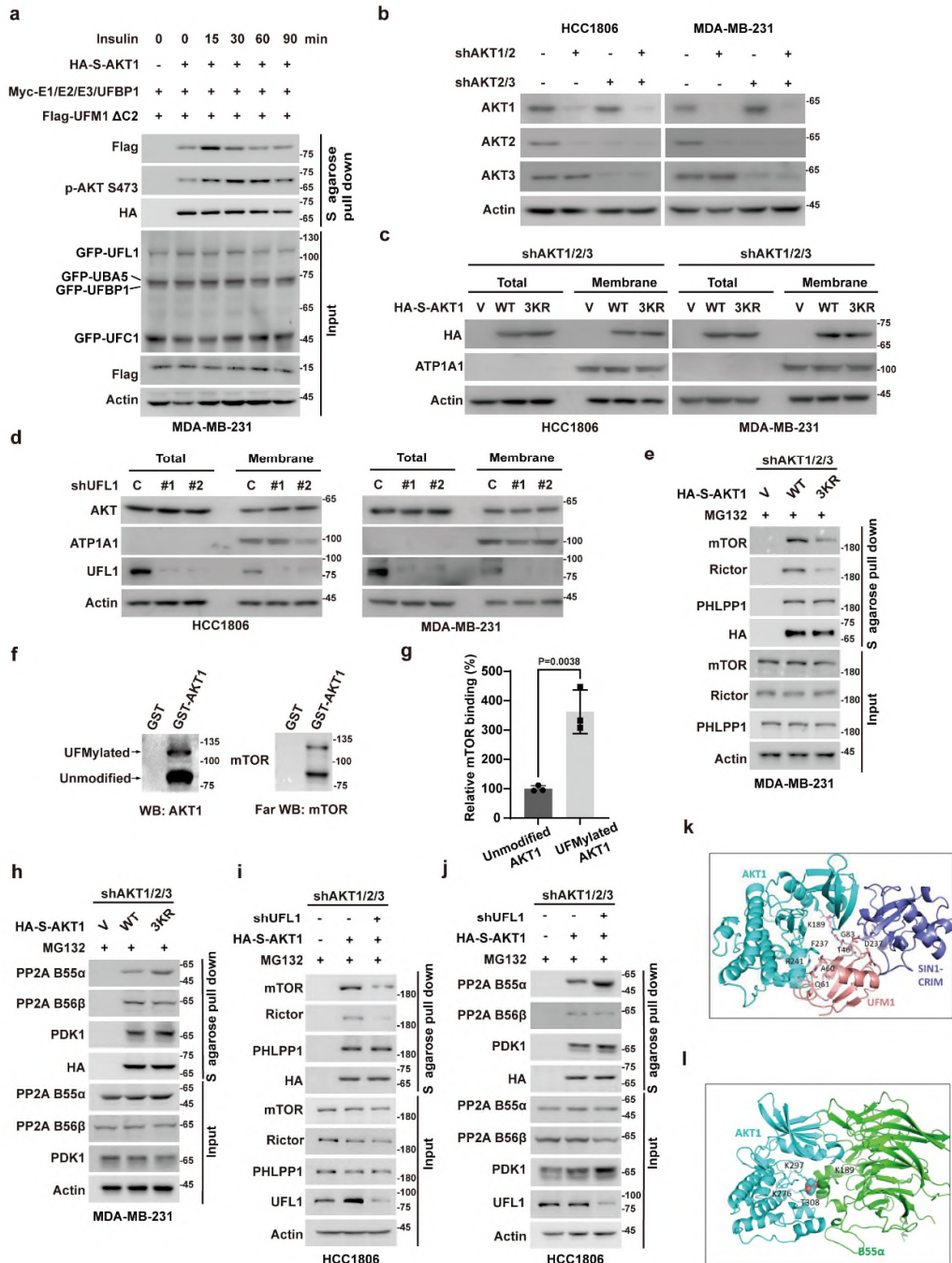
Supplementary Fig. 2 UFL1 promotes TNBC progression via AKT activation.

a, Co-localization of endogenous UFL1 (red) and AKT1 (green) in MDA-MB-231 cells were detected by immunofluorescence (IF) staining. Nuclei were counterstained with DAPI. Scale bars, 10 μ m. The pixel intensity plot for the line was shown in the right panel. **b**, MCF-7, T47D, BT-474 and SK-BR-3 cells stably expressing control or UFL1 shRNAs were generated, and western blotting was performed using the indicated antibodies. **c**, MCF-7, T47D, BT-474 and SK-BR-3 cells were transfected with empty vector or Flag-UFL1. Western blot was performed with indicated antibodies. **d**, MDA-MB-231 and HCC1806 cells were transfected with empty vector or Flag-UFL1 and treated with vehicle or capivasertib (10 μ M) for 24 hours before harvest. Western blotting was performed with indicated antibodies. Source data are provided as a Source Data file.



Supplementary Fig. 3 AKT1 could be ufmylated by UFL1 at Lys189, 276, 297.

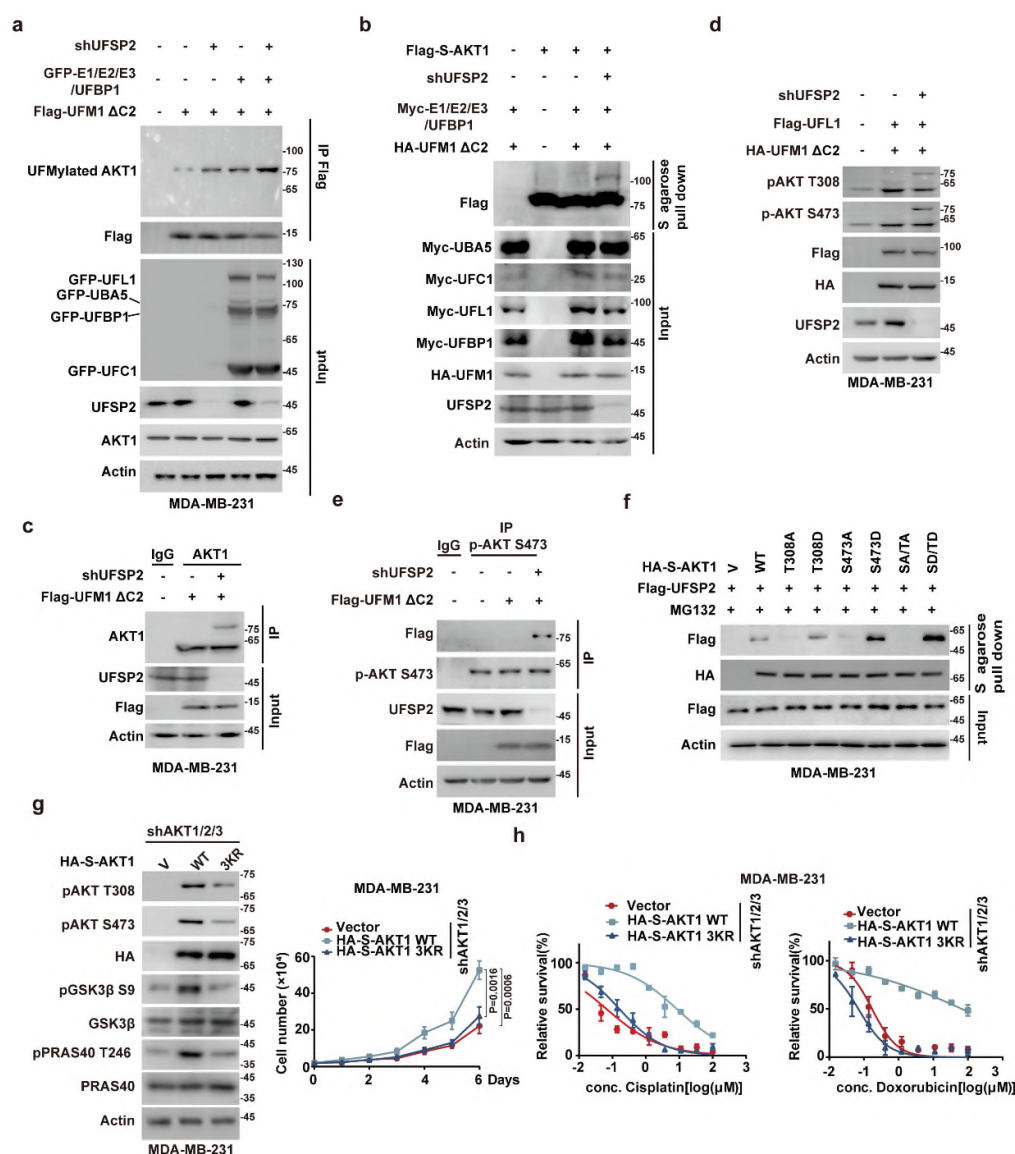
a, Six lysine residues were mutated to arginine in Flag-AKT1 full length, and the UFMylation assay was performed in HEK293T cells. **b**, four lysine residues in AKT1 PH domain were mutated to arginine in Flag-AKT1 full length, and the UFMylation assay was performed. **c-g**, UFMylation assay of the HA-S-AKT1 WT and 3KR was performed in HEK293T (c), MCF-7 (d), T47D (e), BT-474 (f) and SK-BR-3 (g) cells expressing the indicated components of the UFMylation system.



Supplementary Fig. 4 UFMylation promotes AKT1 phosphorylation by enhancing mTORC2 recruitment and restricting PP2A B55α binding.

a, MDA-MB-231 cells were transfected with the indicated plasmids and serum-starved for 16 h, followed by treatment with 100 nM insulin for indicated time periods before

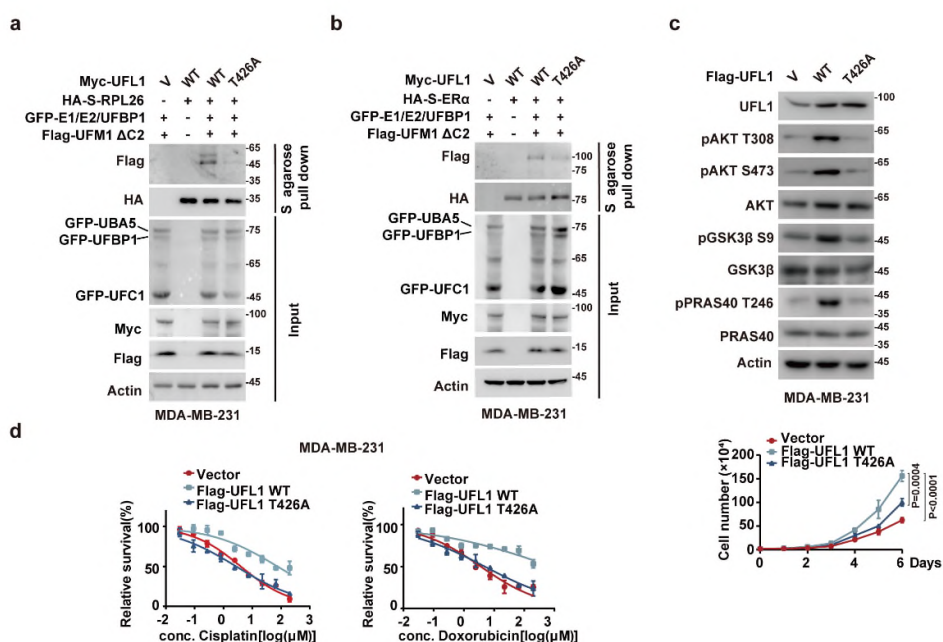
harvest. Cell lysates were pulled down using S-agarose, and then UFMylation and phosphorylation of HA-S-AKT1 were then examined. **b**, HCC1806 and MDA-MB-231 cells stably expressing control, AKT1/2/3 shRNAs were generated, and western blotting was performed using the indicated antibodies. **c**, AKT1/2/3-depleted HCC1806 and MDA-MB-231 cells were transfected with the indicated plasmids, and western blotting was performed as indicated. **d**, HCC1806 and MDA-MB-231 cells stably expressing control or UFL1 shRNAs were generated, and samples of cell fractionations were subjected to western blotting with the indicated antibodies. **e**, MDA-MB-231 cells were transfected with the indicated plasmids and treated with MG132 for 10 hours before harvest. Cell lysates were pulled down using S-agarose, and the interaction between AKT1 and the indicated proteins was then examined. **f**, Purified UFMylation components (His-UBA5, His-UFC1, His-UFL1, His-UFBP1 and His-UFM1 Δ C2) and GST-AKT1 were bacterially expressed and used for in vitro UFMylation reactions with GST-AKT1 as substrate. Reacted GST-AKT1 were separated by SDS-PAGE and transferred to PVDF membrane. After sequential denaturation/renaturation in guanidine-HCl buffers of decreasing concentration, membranes were incubated with Flag-mTOR purified from cells. Bound Flag-mTOR was detected by immunoblotting with anti-mTOR antibody. **g**, Quantitative analysis of relative mTOR binding ratio shows a significant increase in the interaction with UFMylated AKT1 compared to unmodified AKT. **h**, MDA-MB-231 cells were transfected with the indicated plasmids and treated with MG132 for 10 hours before harvest. Cell lysates were pulled down using S-agarose, and the interaction between AKT1 and the indicated proteins was then examined. **i, j** HCC1806 cells were transfected with the indicated plasmids and treated with MG132 for 10 hours before harvest. Cell lysates were pulled down using S-agarose, and the interaction between AKT1 and the indicated proteins was then examined. **k**, Overall structure of the AKT1 (cyan)/SIN1-CRIM (dark blue) complex with UFM1 (pink). **l**, Overall structure of the AKT1 (cyan)-B55 α (green) complex. Data were presented as mean \pm SD of three independent experiments (**g**). Data were analyzed by two-sided one-way ANOVA in (**g**). Source data are provided as a Source Data file.



Supplementary Fig. 5 UFL1-mediated UFMylation activates AKT1 in TNBC.

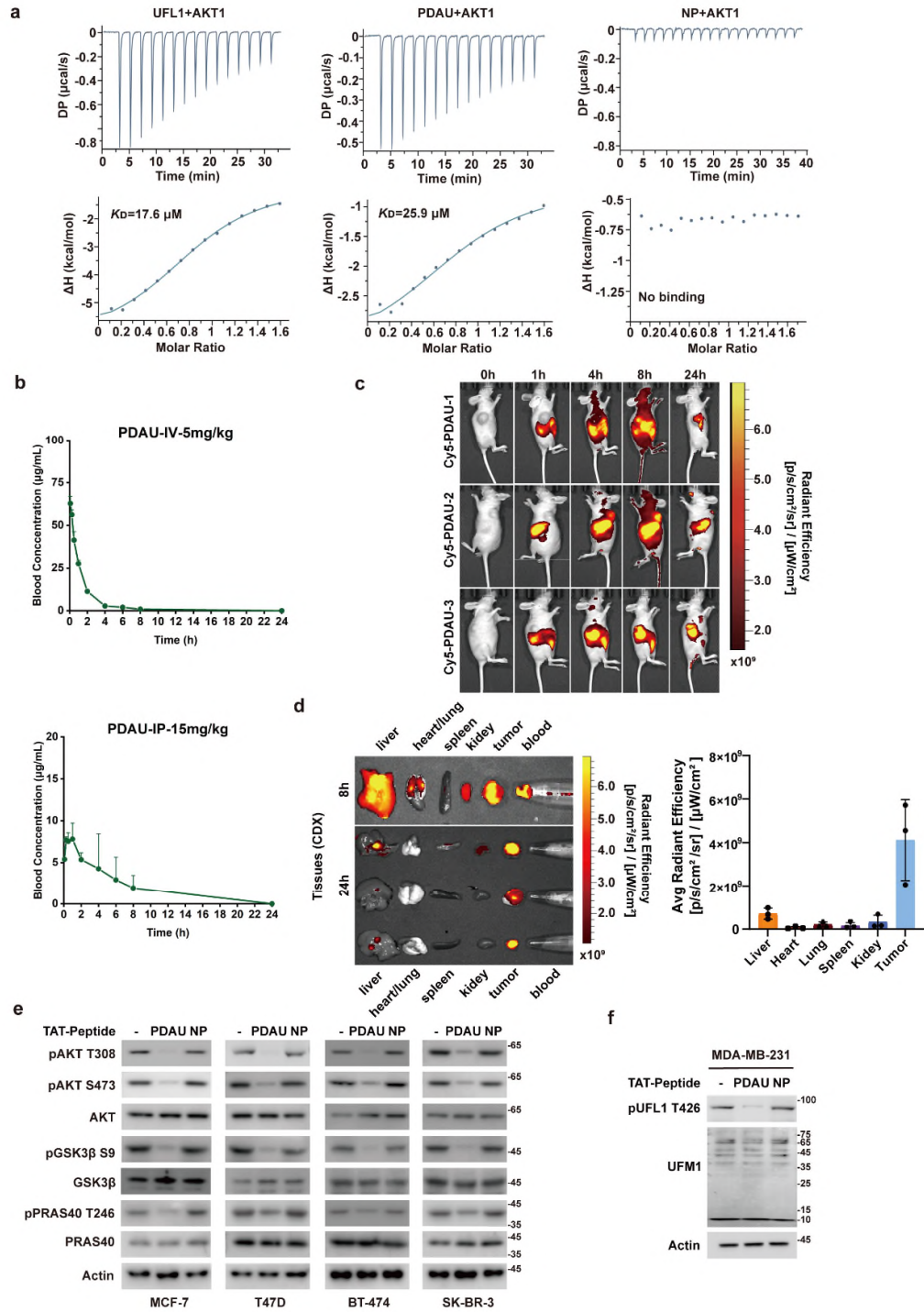
a, MDA-MB-231 cells stably expressing control or UFSP2 shRNA were transfected with the indicated plasmids and UFMylation of endogenous AKT1 was analyzed by immunoprecipitation with an anti-Flag antibody, followed by western blotting using an anti-AKT1 antibody. **b**, UFMylation of AKT1 was analyzed by western blotting using an anti-Flag antibody in HEK293T cells transfected with Flag-S-AKT1 and indicated plasmids. **c**, UFMylation of endogenous AKT1 was analyzed by immunoprecipitation with an anti-AKT1 antibody, followed by western blotting using an anti-AKT1 antibody in MDA-MB-231 cells stably expressing control or UFSP2 shRNA. **d**, MDA-

MB-231 cells were transfected with indicated plasmids, and Western blotting was performed. **e**, UFMylation of endogenous phosphorylated AKT1 (p-AKT S473) was analyzed by immunoprecipitation with an anti-p-AKT S473 antibody, followed by western blotting using an anti-Flag antibody in MDA-MB-231 cells with or without UFS2 depletion and Flag-UFM1 Δ C2 overexpression. **f**, UFMylation of AKT1 was analyzed by western blotting using an anti-Flag antibody in HEK293T cells transfected with Flag-S-AKT1 and indicated plasmids. **g**, AKT1/2/3-depleted MDA-MB-231 cells were transfected with the indicated plasmids, and western blotting was performed as indicated. Cell proliferation was measured. **h**, Cells as in (g) were treated with the indicated concentrations of cisplatin or doxorubicin, and cell survival was determined. Data were presented as mean \pm SD of three independent experiments (**g**, **h**). Data were analyzed by two-sided one-way ANOVA in (**g**). Source data are provided as a Source Data file.



Supplementary Fig. 6 AKT phosphorylates UFL1 at the T426 site to enhance its UFMylation and promote TNBC progression.

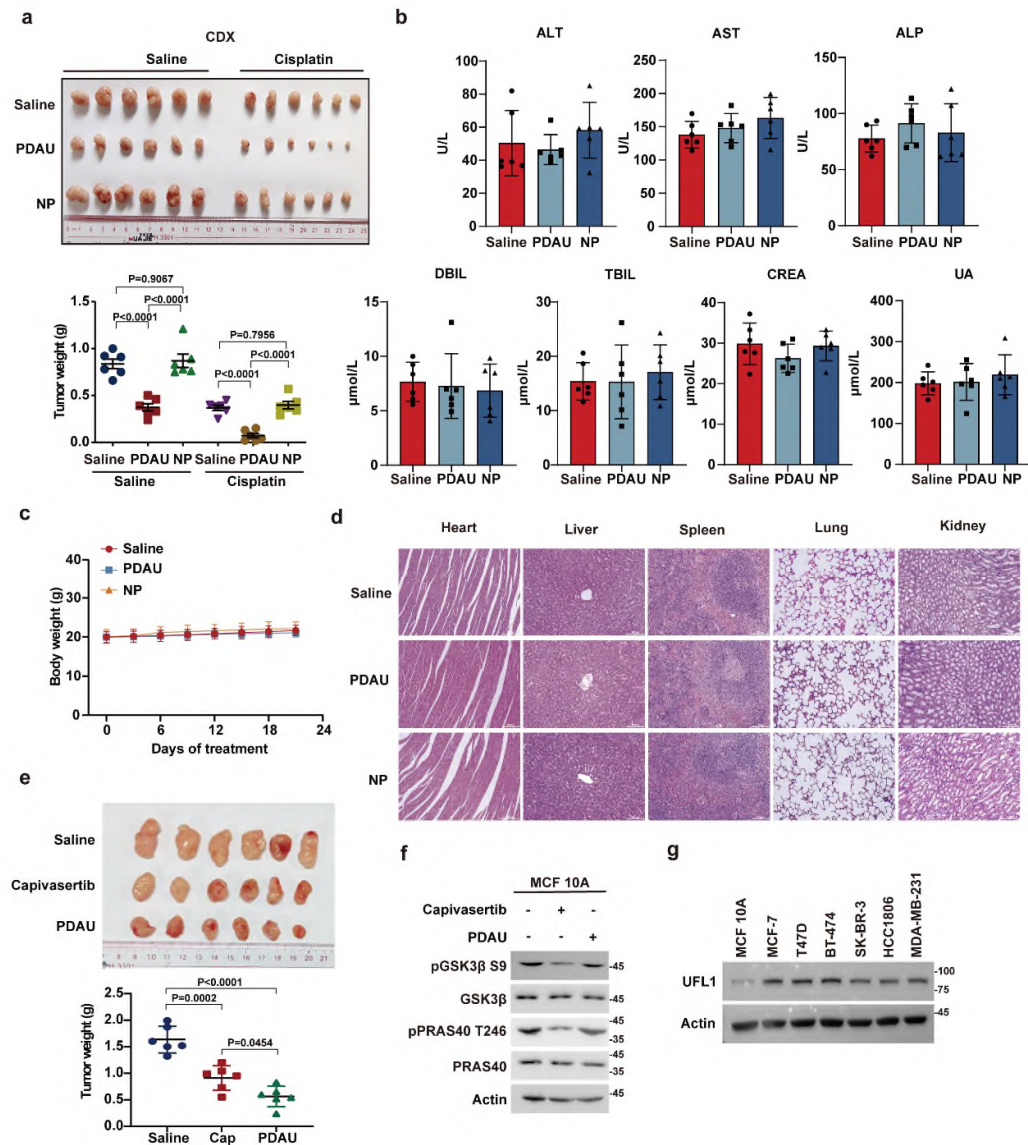
a, UFMylation assay of the HA-S-RPL26 was examined in MDA-MB-231 cells co-transfected with the indicated UFMylation system components. **b**, UFMylation assay of the HA-S-ERα was examined in MDA-MB-231 cells co-transfected with the indicated UFMylation system components. **c**, MDA-MB-231 cells stably expressing vector, Flag-UFL1 WT, or Flag-UFL1 T426A mutant were generated, and western blotting was performed with indicated antibodies. Cell proliferation was measured **d**, MDA-MB-231 cells stably expressing stably expressing vector, Flag-UFL1 WT, or Flag-UFL1 T426A mutant were treated with the indicated concentrations of cisplatin or doxorubicin and cell survival was determined. Data were presented as mean \pm SD of three independent experiments (**c**, **d**). Data were analyzed by two-sided one-way ANOVA in (**c**). Source data are provided as a Source Data file.



Supplementary Fig. 7 Disrupting the UFL1-AKT interaction by PDAU suppresses TNBC progression in vitro.

a, Isothermal titration calorimetry (ITC) measurements showing the binding affinity of AKT1 with UFL1, PDAU and NP. DP, differential power; ΔH , enthalpy change. **b**,

Plasma concentration-vs-time profiles for PDAU in mice following intravenous (IV) administration at a dose of 5 mg/kg or intraperitoneal (IP) administration at a dose of 15 mg/kg. Data represents blood concentration ($\mu\text{g/mL}$) measured at indicated time points. **c**, In vivo fluorescence imaging of mice at 0 h, 1 h, 4 h, 8 h, and 24 h after administration of Cy5-labeled PDAU (Cy5-PDAU). **d**, Ex vivo fluorescence imaging of major tissues and tumors harvested from mice at 8 h and 24 h post Cy5-PDAU administration. Quantitative analysis of fluorescence intensity in major tissues and tumors at 24 h (n=3). **e**, MCF-7, T47D, BT-474 and SK-BR-3 cells were treated with vehicle, PDAU or NP (10 μM) for 24 hours and western blotting was performed indicated antibodies. **f**, MDA-MB-231 cells were treated with vehicle (ddH₂O), PDAU or NP (10 μM) for 24 hours and western blotting was performed indicated antibodies. Source data are provided as a Source Data file.



Supplementary Fig. 8 Disrupting the UFL1-AKT interaction by PDAU suppresses TNBC progression in vivo.

a, Nude mice were subcutaneously inoculated with 2×10^6 HCC1806 cells. Once the xenograft tumors reached a volume of 100 mm^3 , the mice were divided into two groups ($n=6$ per group) and administered either saline or cisplatin (5 mg/kg, once weekly). Tumors were subsequently harvested and weighed. Results represent the mean \pm SD from six mice. **b**, Hepatic and renal functions after peptide treatments were examined by serum-based tests. **c**, Treatment with TAT-peptide did not affect the body weight of the animals. **d**, Representative H&E staining of the heart, liver, spleen, lung, and kidney of mice from (Fig. 7a) that received saline, PDAU or NP treatment. **e**, HCC1806 cells

(2×10^6) were subcutaneously implanted into nude mice ($n = 6$). PDAU (15 mg/kg) was injected intraperitoneally every 2 days and capivasertib (100 mg/kg) was administered by oral gavage once daily for 5 days a week when tumor volume reached 100 mm^3 . Tumors were harvested at endpoint and weighed. Results represent the mean \pm SD from six mice. **f**, MCF 10A cells were treated with vehicle, capivasertib (10 μM) or PDAU (10 μM) for 24 hours and western blotting was performed indicated antibodies. **g**, Western Blot analysis of UFL1 protein expression in various breast cell lines including MCF 10A, and breast cancer cell lines MCF-7, T47D, BT-474, SK-BR-3, HCC1806, and MDA-MB-231. Data were analyzed by two-sided one-way ANOVA in (**a**, **e**). Source data are provided as a Source Data file.

Supplementary Table 1.

| NO. | AUC _(0-t) | AUC _(0-∞) | MRT _(0-t) | MRT _(0-∞) | <i>t</i> _{1/2z} | V _z | CL _z | C _{max} |
|------|----------------------|----------------------|----------------------|----------------------|--------------------------|----------------|-----------------|------------------|
| | h*µg/mL | h*µg/mL | h | h | h | mL/kg | mL/min/kg | µg/mL |
| 1 | 87.78 | 90.35 | 1.33 | 1.58 | 1.31 | 104.88 | 0.922 | 67.61 |
| 2 | 85.55 | 86.33 | 1.30 | 1.38 | 1.13 | 94.47 | 0.965 | 60.75 |
| 3 | 84.51 | 86.26 | 1.53 | 1.70 | 1.43 | 119.88 | 0.966 | 60.04 |
| Mean | 85.95 | 87.65 | 1.39 | 1.55 | 1.29 | 106.41 | 0.951 | 62.80 |
| SD | 1.67 | 2.34 | 0.12 | 0.16 | 0.15 | 12.78 | 0.025 | 4.18 |

Table S1. Pharmacokinetic Parameters after Intravenous Administration

Supplementary Table 2.

| NO. | AUC _(0-t) | AUC _(0-∞) | MRT _(0-t) | MRT _(0-∞) | <i>t</i> _{1/2z} | T _{max} | C _{max} | F |
|------|----------------------|----------------------|----------------------|----------------------|--------------------------|------------------|------------------|-------|
| | µg/mL*h | µg/mL*h | h | h | h | h | µg/mL | % |
| 1 | 56.08 | 71.67 | 3.58 | 5.49 | 3.02 | 1.00 | 10.00 | 21.75 |
| 2 | 28.27 | 36.46 | 2.85 | 5.11 | 3.40 | 0.25 | 7.27 | 10.96 |
| 3 | 21.59 | 25.62 | 2.05 | 4.08 | 4.80 | 0.25 | 8.08 | 8.37 |
| Mean | 35.31 | 44.58 | 2.83 | 4.89 | 3.74 | 0.50 | 8.45 | 13.70 |
| SD | 18.29 | 24.08 | 0.76 | 0.73 | 0.94 | 0.43 | 1.40 | 7.09 |

Table S2. Pharmacokinetic Parameters after Intraperitoneal Administration